The conserved positive charge in the transmembrane domain of HIV gp41 contributes to its trimerization

Timothy M. Reichart[1]†, Daniel P. Leaman[2], Daniel I. Sands[2], Michael B. Zwick[2*], and Philip E. Dawson[1*].

[1]Department of Chemistry, The Scripps Research Institute, 10550 North Torrey Pines Road, La Jolla, CA 92037

[2]Department of Immunology and Microbiology, The Scripps Research Institute, 10550 North Torrey Pines Road, La Jolla, CA 92037

†Present address: Swiss Institute for Experimental Cancer Research, School of Life Sciences, Ecole Polytechnique Fédérale de Lausanne, Switzerland.

*: Co-corresponding authors

Abstract:

The transmembrane (TM) domain of HIV glycoprotein gp41 anchors the envelope (Env) spike in the viral membrane and is highly conserved. The mid-span arginine 696 is particularly conserved, and the only other residue found in this position is lysine. Seeking to examine the role of this conserved positive charge in the structure and function of the gp41 TM domain, we synthesized a series of peptides corresponding to this region. Analysis of the peptides in a previously validated fluorescence assay in model membranes showed that the native TM domain is trimeric. Peptides in which the intramembrane arginine was mutated to alanine showed significantly lower trimerization propensity. In contrast, this mutation in the context of infectious pseudovirus caused only modest decreases in viral stability and infectivity. We propose a model to explain the importance of this charge to gp41 structure and to HIV infection.

Graphical Abstract:

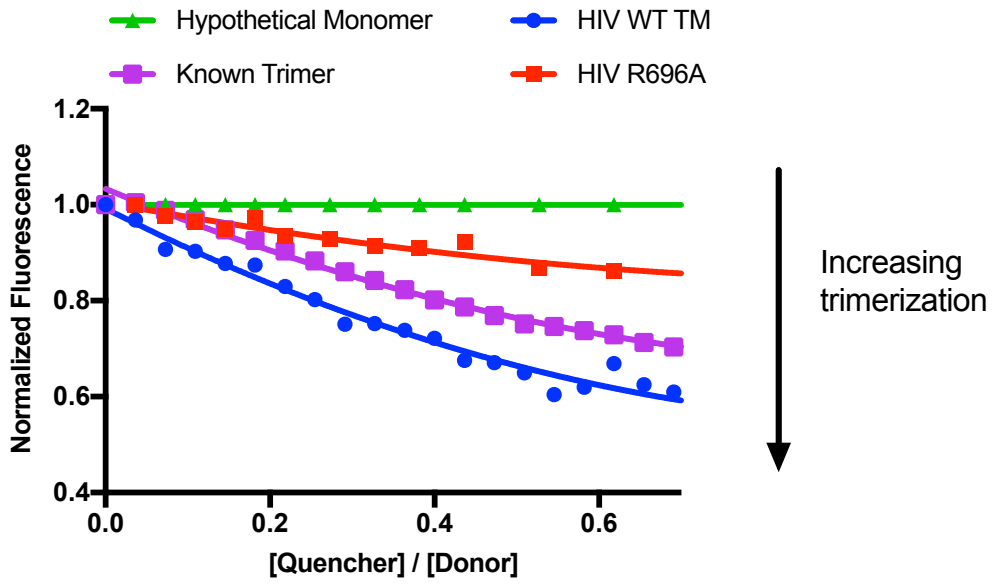

Introduction

The HIV envelope glycoprotein (Env) spike is a trimer of gp120 and gp41 subunits $(gp120\text{-}gp41)_3$ and is essential for virus entry into host cells.[1-3] Recent work demonstrated the importance of the transmembrane (TM) domain of gp41 in modulating both the structure of the adjacent membrane-proximal external region (MPER) and the recognition of the MPER by broadly neutralizing antibodies.[4-8] The TM domain of gp41 is highly conserved (Figure 1A), suggesting its importance to the structure and function of gp41. A role of the TM in intracellular trafficking of Env has also been demonstrated.[9,10] Peculiarly, there is a very highly conserved arginine at position 696 (97.2% of 1937 sequences), in the middle of the TM domain. In every case where arginine is not found, the substitution is a lysine that has a positive charge at physiological pH. The presence of a positive charge into the middle of a membrane is strongly energetically unfavorable,[11] suggesting the existence of a strong evolutionary pressure to retain this residue. Arg 696 has been suggested to play a structural role in trimerization by forming polar contacts within the membrane, either alone or in combination with a GxxxG motif, and computational studies on the gp41 TM domain support this claim.[9,12-14]

Biophysical studies on the HIV TM have yielded inconsistent results on the oligomeric state of this domain. An NMR analysis of a TM peptide in a DMPC/DHPC mixed micelle showed no evidence of trimerization, but the specific transmembrane peptide used in that study contained significant portions of the MPER and cytoplasmic tail.[15] A longer MPER-TM-CT construct in dodecylphosphocholine micelles was found to be monomeric in analytical ultracentrifugation studies, but addition of adjacent domains resulted in trimer formation.[16] In contrast, an earlier NMR study reported that the transmembrane domain forms well-ordered trimers with a three-chain coiled-coil from residues 686 to 696, stabilized by a network of polar contacts in the cytoplasmic tail.[8]

Previous studies on the structure and function of the TM domain were either structural studies of much longer constructs with larger potential interfaces or computational studies without direct experimental evidence. To bridge this gap and to probe the importance of this residue in oligomerization, we chemically synthesized several peptides containing fluorophores and analyzed them in model membranes using a previously-validated[17] fluorescence-based oligomerization assay. We also examined the functional effects of mutating this residue in the context of single-cycle infectious pseudoviruses in order to gain a better understanding of the role of R696.

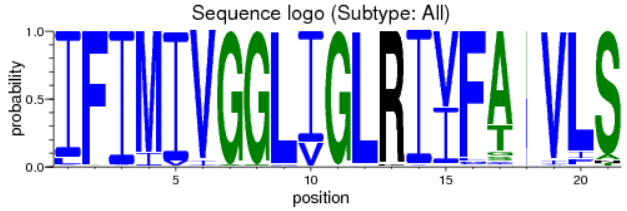

(b)

1	LWYIK-IFIMIVGGLVGLRIVFAVL-SIVNRVR
2	-IFIMIVGGLVGLRIVFAVL-SIVNRV
3	-IFIMIVGGLVGL**R**IVFAVL-SIVNRVKKKK
4	-IFIMIVGGLVGL**A**IVFAVL-SIVNRVKKKK
5	-LLIAVLLLVIANLILLIAV-ARLRYL

Figure 1. The conserved HIV-1 gp41 TM domain (a) A LogoPlot of the transmembrane (TM) domain of HIV gp41 sourced from the Los Alamos HIV sequence database[18] shows its high sequence conservation; (b) Sequences of peptides used in this study. Each peptide was synthesized in N-terminal NBD, N-terminal TAMRA, and unlabeled variants.

Results

Several series of peptides corresponding to the TM domain of gp41 were synthesized using standard Boc/t-butyl solid-phase peptide synthesis (Figure 1B). Each peptide series contained three variants: one with a free N terminus, one with a nitrobenzodiazole (NBD) as a membrane-specific fluorescent dye, and with a tetramethylrhodamine (TAMRA) dye which quenches NBD fluorescence upon close association. Each peptide series was tested in a fluorescence assay to measure oligomerization. Briefly, dissolution of the peptides in 2 or 4 mM of the detergent C14 betaine (3-(N,N-dimethylmyristylammonio)propane sulfonate, above the CMC), presented the peptides in micelles previously shown to be accurate mimics of membranes for the analysis of oligomerization states of TM domains.[17] Addition of the quenching **TAMRA** peptide concomitant with the equal removal of unlabeled peptide (thus maintaining a constant concentration of **2-NBD** and all peptides) results in a decrease of NBD fluorescence if the peptides are closely associated.

Peptides in series **1** correspond to gp41(679-708), and are similar in length to those used in previous NMR studies of the TM domain.[8,15] Surprisingly, these peptides did not show a decrease in NBD fluorescence upon titration of the TAMRA-labeled peptide, but instead showed a mild increase in fluorescence. However, further experiments revealed that the fluorescence parameters of **1-NBD** did not match those of the NBD fluorophore in a hydrophobic membrane environment, but instead matched the fluorescence parameters corresponding to the NBD fluorophore in an aqueous environment (Figure S1), suggesting that the α-helix of the TM domain continues to propagate out of the membrane in such a way that a fluorophore five residues away from the membrane is unable to contact the hydrophobic portion of the membrane. Intriguingly, this fits the NMR data of a similar length construct that suggested a continuous, helical, monomeric TM domain[15], which would place the NBD group outside of the membrane and in the aqueous environment.

To ensure that the NBD group was properly positioned in the membrane and thus had the requisite fluorescence parameters, a second-generation peptide series **2** was designed that removed the five residues of the MPER. Peptide **2-NBD** had a maximum excitation at $\lambda = 466$ nm and maximum emission at $\lambda = 534$ nm (Figure S2), and a significantly higher fluorescence intensity, which are evidence that the NBD group of **2-NBD** could be located in the hydrophobic portion of the membrane mimic. When the quenching peptide **2-TAMRA** was added to a solution of **2-NBD** in C14 betaine along with the simultaneous removal of unlabeled **2**, the NBD fluorescence decreased in a dose-dependent manner. This decrease in fluorescence fits a monomer-trimer equilibrium that is neither explained by monomer alone nor by a monomer-dimer equilibrium (Figure 2). Introducing a parameter for a monomer-dimer-trimer equilibrium does not improve the fit. These data were used to calculate an equilibrium constant for peptide trimerization of 2.7×10^{-8} MF^2, using MF = mole fraction of peptide / detergent as the appropriate description of concentration.[19]

Although the peptides in series **2** provide good support for a trimeric self-association of the HIV gp41 TM domain, these peptides exhibited low solubility that resulted in noisy data when working at the limits of solubility, and precluded future experiments that require high concentrations of peptide. A more soluble series of peptides **3** were designed and synthesized with four C-terminal lysine residues to enhance solubility. These peptides had higher aqueous

and micellar solubility and provided cleaner fluorescence spectra than the corresponding peptides in series **2**. In the fluorescence assay of oligomerization described above, peptide **3** showed results consistent with a monomer-trimer equilibrium similar to the less-soluble peptides **2** albeit with a slightly reduced equilibrium constant of 2.8×10^{-7}. Next, a series of peptides **4** in unlabeled, NBD, and TAMRA forms with the R696A mutation were synthesized and used in the same assay. These peptides were still best described using a monomer-trimer equilibrium model (Figure 2A), but showed a markedly reduced propensity for trimerization with equilibrium constant 1.3×10^{-6}. The difference in equilibria constants for peptides **3** and **4** corresponds to a free energy difference of 3.8 kJ • mol^{-1}. For both peptides **3** and **4**, a fit of the data describing a monomer-dimer equilibrium shows large residuals with a noticeable quadratic pattern–a clear indication that the model is underfitting the data (Figure 2B). In contrast, a model describing a monomer-trimer equilibrium has smaller residuals apparently randomly scattered around 0, suggesting a much better fit (Figure 2B).

To validate this assay, we synthesized a series of peptides **5** that used the designed synthetic trimeric TM domain peptides described by DeGrado and colleagues[22] and subjected them to the same fluorescence assay of oligomerization. As expected, we observed results consistent with a monomer-trimer equilibrium and quite similar to peptides in series **2, 3,** and **4** (Figure 2A).

Since the R696A mutation reduced the propensity for TM trimerization, we probed its effect on the stability and function of HIV-1 Env in the context of single-round infectious pseudoviruses. Envs from four isolates were studied: the clade A BG505, the clade B JRFL, and the clade C isolates CH505 and COT6, the latter of which contains a rare natural K696. The A696 mutant Env viruses showed no significant differences in stability compared to wild-type viruses when measured by the reduction in infectivity through exposure to elevated temperature (Figure 3A; Table 1). We also measured the stability of the mutant Env pseudoviruses using another assay of infectivity decay at 37 °C. The mutant Env pseudoviruses showed variable effects depending on the isolate. The R696A mutants of BG505 and JRFL showed no significant differences in infectivity relative to wild-type over a 72-hour time course (Figure 3B; Table 1). Notably however, the relatively stable COT6 isolate became more stable when K696 was mutated to an alanine ($t_{1/2}$ increased from 21.3 hours to 37.1 hours), while the less stable CH505 isolate showed decreased stability over time from the R696A mutation ($t_{1/2}$ reduced 50% from 20.2 hours to 10.4 hours).

Two of the four isolates showed statistically significant, diminished relative infectivity due to the mutation R696A (Figure 3C). Notably, the isolate whose infectivity was reduced most by R696A, CH505, was also the least stable of the four isolates to begin with (Table 1), and the only one destabilized by R696A in the 37˚C stability assay (Figure 3B). These results suggest a possible role of R696 in interactions distributed throughout the Env trimer that preserve its overall stability and function.

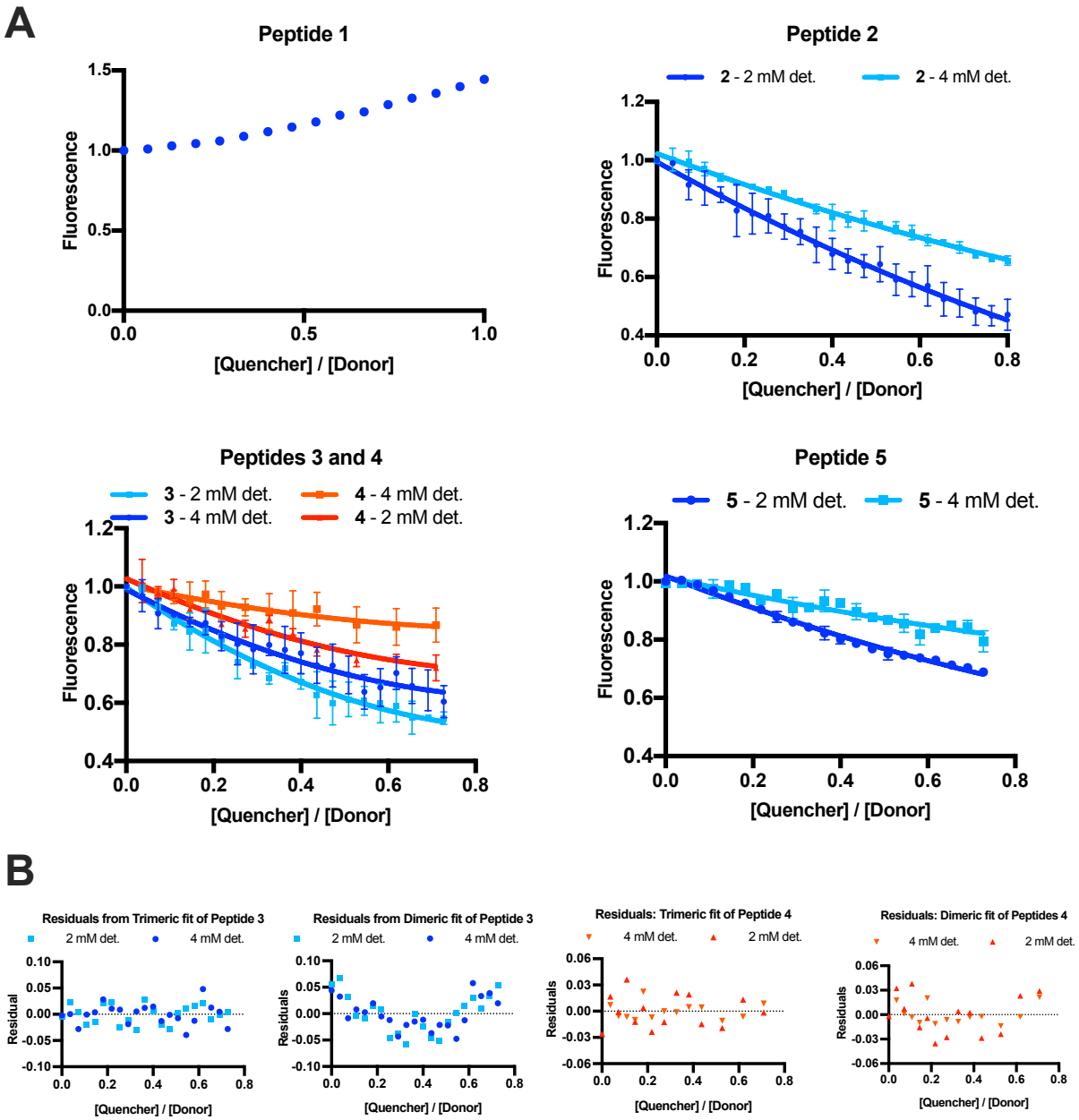

Figure 2: Oligomerization analysis of HIV TM peptides by fluorescence titration assays. A: Fluorescence quenching in micelles shows the trimeric nature of the TM domain of gp41 in peptides 2, 3, and 4, and an equilibrium shifted towards monomer in the R696A containing peptide 4. B: The residuals show that a monomer-dimer equilibrium does not fit the data, but a monomer-trimer equilibrium fits well.

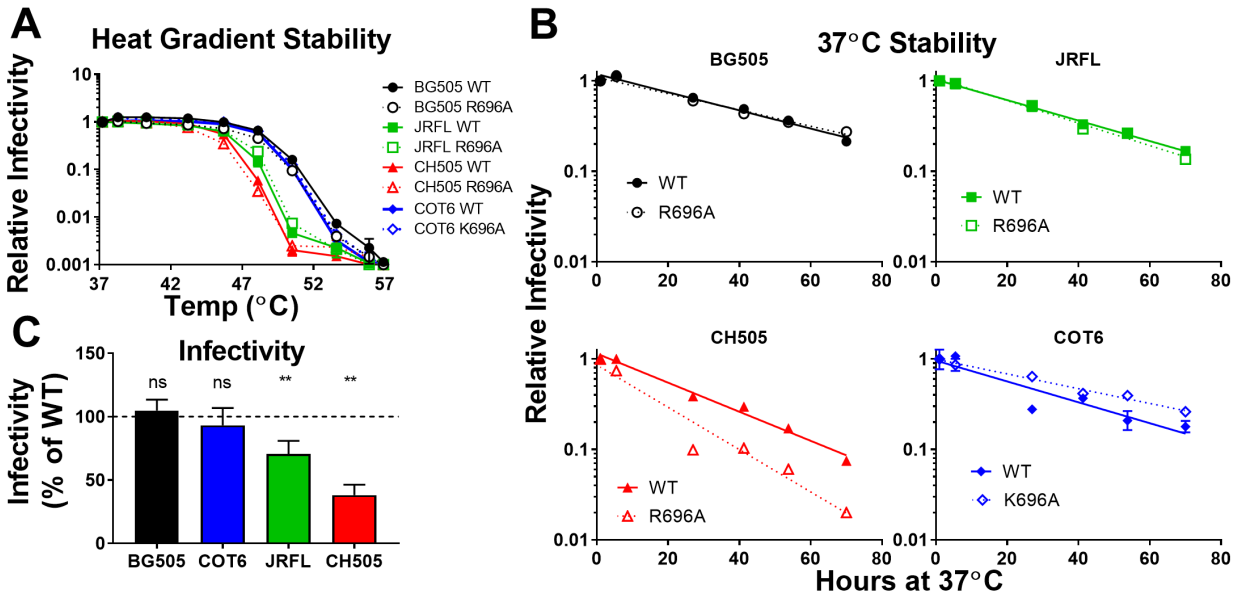

Figure 3: Effects on HIV-1 Env infectivity and stability by Ala mutation at Env position 696 in the gp41 TM domain. a) T_{90}, or the temperature at which infectivity is reduced by 90% in a 1 h incubation period, of wild-type and R/K696A mutant pseudovirus are not statistically different across a range of isolates; b) Stability as measured by infectivity retained over time at 37 °C is unchanged by the R/K696A substitution for JRFL and BG505 isolates, increased for COT6, and decreased for CH505 as compared to wild-type of the same isolate; c) Infectivity of R/K696A mutants is significantly reduced for two of four isolates tested (p values: ns = not significant, ** ≤ .01).

Table 1. Effect on HIV-1 Env functional stability by Ala mutation at gp41 position 696.

	BG505		JRFL		CH505		COT6	
	WT	R696A	WT	R696A	WT	R696A	WT	K696A
T_{90}*	50.9	51.3	48.8	49.4	47.6	47.5	50.7	50.6
$t_{1/2}$†	32.9	32.9	26.4	25.2	20.2	10.4	21.3	37.1

* T90 is the temperature at which infectivity is reduced by 90% in a 1 h incubation period (Figure 3A).
† $t_{1/2}$ is the half-life of viral infectivity retained at 37 ˚C (Figure 3B).

Discussion

Chemical synthesis of fluorescently tagged peptides corresponding to the HIV gp41 TM domain enabled the study of the TM peptide oligomerization state in model membranes. The dose-dependent decrease in fluorescence upon the addition of a quenching fluorophore matched that of a monomer-trimer equilibrium, without showing evidence of a dimer intermediate. These data suggest that the TM domain of gp41 energetically favors a trimer in the absence of the rest of the protein. Replacing the arginine buried in the membrane with an alanine also resulted in a monomer-trimer equilibrium but with the equilibrium shifted towards monomer. The difference in equilibria constants corresponds to a free energy difference of 3.8 kJ • mol^{-1}. Thus, arginine

696 contributes to trimer formation but is not the sole determinant. Peptide **1**, which included five residues of the MPER, did not show this behavior. Because of the low fluorescence signal, this is not strong evidence for a preference for monomer in membranes, although the data is consistent with this interpretation and could potentially help explain the disparities between the structures suggested by different NMR studies.

When the R696A mutation was made in the context of whole Env on virus, the modest free energy change of the gp41 TM domain corresponded to variable changes in Env structure and function. Of the four isolates studied, two had significantly reduced infectivity when arginine 696 was mutated to alanine. Notably, the isolate whose infectivity was most affected by the mutation was also destabilized by the mutation at physiological temperature. Thus, perturbations to the TM domain trimer tend to also reduce HIV-1 infectivity. This relationship can be explained as a stabilization of the unliganded state relative to the CD4-bound state, matching the conclusion from the peptide fluorescence assays, or from a destabilization of the CD4-bound state, or there may be other possibilities. This fine-tuned intramolecular interaction, coupled with the high conservation of the TM domain, suggests a functional role for the TM domain in virus infectivity. Extensive structural rearrangements of gp41 occur after CD4 engagement of the target cell and dissociation of the gp120 subunit.[20-22] The energetically favorable six-helix bundle formation in the extracellular domains of gp41, for example, requires significant structural rearrangements that lead to viral fusion.[23,24]

In the context of full length Env, the R696A mutation did not result in profound or uniform effects on sensitivity to thermal denaturation or on infectivity decay at physiological temperature. Two Env variants showed comparable rates of infectivity decay at 37 °C, suggesting a similar activation energy towards degradation of the unliganded state into nonfunctional spikes. Of note, the degradation of Env spikes to nonfunctional spikes is irreversible (i.e. not an equilibrium process) and the energetic landscape may vary depending on the particular isolate of HIV studied. Our observations that the COT6 isolate was stabilized slightly at 37 °C by the K696A mutation and was also thermally stable with a high T_{90}, imply a higher activation energy barrier that limits non-productive conformations of Env. Conversely, the less stable CH505 may have a lower activation energy toward such nonfunctional states. This reduced stability of CH505 R696A was observed experimentally as a reduced infectivity half-life at 37 °C.

We propose that the TM domain in the viral membrane acts as a reservoir of potential energy that contributes to the series of structural rearrangements upon engagement of the virus with CD4 on the target cell and that disruption of these interactions may reduce or abrogate viral infectivity in an Env dependent manner. Our work suggests that the conserved positive charge at position 696 helps promote trimerization of this domain. The wild-type TM domain in model membranes exists in equilibrium between monomeric and trimeric states, with the trimeric form favored under physiological conditions. Previous reports suggest that the folded structure of the trimeric Env spikes require each gp41 TM domain to be spatially distal from the others in the unliganded state of the virus[3], but form a tight trimer in the CD4-bound state.[8] The energetic penalty of positioning an arginine in an isolated, membrane-embedded TM domain is at least partially relieved by trimerization, providing an element of the driving force for the gp41 rearrangements that ultimately lead to viral fusion.

Conclusions

This work suggests that the latent potential for trimerization contained in the TM domain of HIV gp41 is an important energetic reservoir for necessary structural rearrangements in Env required for HIV-1 infection. The conserved positive charge at position 696, which is typically energetically disfavored in membranes, contributes to this potential energy by destabilizing the monomeric state of the TM compared to the trimeric state. Draining this reservoir of potential energy via mutation to alanine may reduce infectivity of HIV virions in a subset of isolates.

Materials and Methods

Peptide Synthesis. Peptides were synthesized as C-terminal amides via solid phase peptide synthesis with N-*tert*-butoxycarbonyl (Boc) protected amino acids and 4-methylbenzhydrylamine (MBHA) resin, on a 0.20 mmol scale. The standard 20-minute coupling cycle used a five-fold molar excess of amino acid and HCTU and a nine-fold molar excess of DIEA in DMF. Crude peptides were cleaved from resin and side chains were deprotected by treatment with anhydrous hydrofluoric acid with 10% anisole as scavenger. Peptides were purified by reverse-phase HPLC and analyzed by reverse-phase HPLC and ESI-MS.

7-nitrobenzofuran (NBD) was coupled to the N-terminus of peptides by the addition of 4-chloro-7-nitrobenzofuran (NBD-Cl) to resin in the presence of 1 equivalent of DIEA for at least one hour. Tetramethylrhodamine (TAMRA) was coupled to the N-terminus of peptides by dissolving 1.2 equivalents of 5(6)-carboxytetramethylrhodamine in minimal dichloromethane (DCM), activation with 1.15 equivalents of a 0.5 M solution of HCTU in DMF and 3 equivalents of DIEA, and adding that mixture to the resin for at least one hour.

Fluorescence-based Determination of Oligomerization State of HIV gp41 TM Peptides. A 1:1 ratio of unlabeled peptide to NBD-labeled peptide (2.75 μM each) was dissolved in 2.0 mM of the detergent C-14 betaine (3-(N,N-dimethylmyristylammonio)propanesulfonate). The solution was excited at 460 nm with a bandwidth of 2 nm, and the fluorescence was monitored at 525 nm. After each measurement, some of the solution was removed and an equal amount of a 1:1 solution of NBD-labeled peptide and TAMRA-labeled peptide was added. This kept the total concentration of peptide constant, kept the concentration of the NBD-labeled peptide constant, but increased the concentration of the TAMRA-labeled peptide. As the concentration of the TAMRA increases, the fluorescence of the NBD group at 525 nm decreases as a function of the oligomerization state of the peptide. Fluorescence curves were evaluated using Prism version 7.0 (Graphpad, CA) using models for monomer, dimer, trimer, and higher order oliogmers as previously described.[25]

Virus production and infectivity measurement. HIV-1 pseudotyped virus was generated by co-transfection of 293T cells with Env plasmid DNA and the HIV-1 backbone plasmid pSG3ΔEnv using 25kDa polyethylene imine (PEI), as previously described.[26] Envs for HIV isolates JRFL and BG505 were obtained from from D. Burton (Scripps), COT6 from L. Morris (U. Witwatersrand), and CH505 was synthesized by Genscript. BG505 and COT6 were expressed from the pSVIII plasmid, JRFL was contained in the pcDNA3.1 plasmid, and CH505 was in pLenti-III plasmid. Mutations to amino acid 696 were introduced using the Quickchange Site-directed Mutagenesis Kit (Agilent). To measure viral infectivity, varying dilutions of virus were added to $CD4^+CXCR4^+CCR5^+$ TZM-bl target cells. Following a 72 hour incubation at 37 °C, cells were lysed, Bright-Glo luciferase reagent (Promega) was added, and luminescence in relative light units (RLUs) was measured using a Synergy H1 plate reader (BioTek).

HIV temperature gradient stability assay. HIV Env stability assays were performed as previously described.[27] Briefly, virus samples were exposed to a thermal gradient from 37 to 57ºC for 1 h on a gradient PCR block. Following heat treatment, infectivity was determined by adding virus to TZM-bl cells and measuring luciferase. For determination of T_{90}, RLU data were background-subtracted using RLU from uninfected cells, normalized according to the 37ºC data point, and the temperature corresponding to 90% reduction of infectivity was determined by non-linear regression using Prism version 7.0 software (Graphpad, CA).

HIV stability at 37ºC. HIV samples were incubated at 37˚C for different time points and then frozen at –80°C. Virus was synchronously thawed and HIV-1 infectivity was determined using TZM-bl cells as described above. The time corresponding to 50% reduction of infectivity relative to t_0 (half-life) was determined using Prism version 7.0 software (Graphpad, CA).

Acknowledgements

This research was supported by the California HIV/AIDS Research Grant Program, D10-SRI-30 (T.M.R.), International AIDS Vaccine Initiative (P.E.D.), and NIH AI114401 and AI143563 (M.B.Z.) and GM098871 (P.E.D.). We thank Arthur S. Kim for technical help with early experiments.

References

1. Julien J-P, Cupo A, Sok D, Stanfield RL, Lyumkis D, Deller MC, Klasse P-J, Burton DR, Sanders RW, Moore JP and others. Crystal Structure of a Soluble Cleaved HIV-1 Envelope Trimer. Science 2013;342(6165):1477-1483.
2. Liu J, Bartesaghi A, Borgnia MJ, Sapiro G, Subramaniam S. Molecular architecture of native HIV-1 gp120 trimers. Nature 2008;455(7209):109-U76.
3. Lyumkis D, Julien J-P, de Val N, Cupo A, Potter CS, Klasse P-J, Burton DR, Sanders RW, Moore JP, Carragher B and others. Cryo-EM Structure of a Fully Glycosylated Soluble Cleaved HIV-1 Envelope Trimer. Science 2013;342(6165):1484-1490.
4. Montero M, Gulzar N, Klaric K-A, Donald JE, Lepik C, Wu S, Tsai S, Julien J-P, Hessell AJ, Wang S and others. Neutralizing Epitopes in the Membrane-Proximal External Region of HIV-1 gp41 Are Influenced by the Transmembrane Domain and the Plasma Membrane. Journal of Virology 2012;86(6):2930-2941.
5. Reichart TM, Baksh MM, Rhee JK, Fiedler JD, Sligar SG, Finn MG, Zwick MB, Dawson PE. Trimerization of the HIV Transmembrane Domain in Lipid Bilayers Modulates Broadly Neutralizing Antibody Binding. Angew Chem Int Ed Engl 2016;55(8):2688-92.
6. Alam SM, Morelli M, Dennison SM, Liao H-X, Zhang R, Xia S-M, Rits-Volloch S, Sun L, Harrison SC, Haynes BF and others. Role of HIV membrane in neutralization by two broadly neutralizing antibodies. Proceedings of the National Academy of Sciences of the United States of America 2009;106(48):20234-20239.
7. Song LK, Sun ZYJ, Coleman KE, Zwick MB, Gach JS, Wang JH, Reinherz EL, Wagner G, Kim M. Broadly neutralizing anti-HIV-1 antibodies disrupt a hinge-related function of gp41 at the membrane interface. Proceedings of the National Academy of Sciences of the United States of America 2009;106(22):9057-9062.
8. Dev J, Park D, Fu Q, Chen J, Ha HJ, Ghantous F, Herrmann T, Chang W, Liu Z, Frey G and others. Structural basis for membrane anchoring of HIV-1 envelope spike. Science 2016;353(6295):172-175.
9. Miyauchi K, Curran AR, Long Y, Kondo N, Iwamoto A, Engelman DM, Matsuda Z. The membrane-spanning domain of gp41 plays a critical role in intracellular trafficking of the HIV envelope protein. Retrovirology 2010;7(1):95.

10. Teese MG, Langosch D. Role of GxxxG Motifs in Transmembrane Domain Interactions. Biochemistry 2015;54(33):5125-5135.
11. Wimley WC, White SH. Experimentally determined hydrophobicity scale for proteins at membrane interfaces. Nature Structural Biology 1996;3(10):842-848.
12. Oakes V, Torralba J, Rujas E, Nieva JL, Domene C, Apellaniz B. Exposure of the HIV-1 broadly neutralizing antibody 10E8 MPER epitope on the membrane surface by gp41 transmembrane domain scaffolds. Biochimica Et Biophysica Acta-Biomembranes 2018;1860(6):1259-1271.
13. Molinos-Albert LM, Bilbao E, Agullo L, Marfil S, Garcia E, Luisa Rodriguez de la Concepcion M, Izquierdo-Useros N, Vilaplana C, Nieto-Garai JA, Contreras FX and others. Proteoliposomal formulations of an HIV-1 gp41-based miniprotein elicit a lipid-dependent immunodominant response overlapping the 2F5 binding motif. Scientific Reports 2017;7.
14. Hollingsworth LR, Lemkul JA, Bevan DR, Brown AM. HIV-1 Env gp41 Transmembrane Domain Dynamics Are Modulated by Lipid, Water, and Ion Interactions. Biophysical Journal 2018;115(1):84-94.
15. Chiliveri SC, Louis JM, Ghirlando R, Baber JL, Bax A. Tilted, Uninterrupted, Monomeric HIV-1 gp41 Transmembrane Helix from Residual Dipolar Couplings. Journal of the American Chemical Society 2018;140(1):34-37.
16. Dai Z, Tao Y, Liu N, Brenowitz MD, Girvin ME, Lai JR. Conditional Trimerization and Lytic Activity of HIV-1 gp41 Variants Containing the Membrane-Associated Segments. Biochemistry 2015;54(8):1589-1599.
17. Gratkowski H, Lear JD, DeGrado WF. Polar side chains drive the association of model transmembrane peptides. Proceedings of the National Academy of Sciences of the United States of America 2001;98(3):880-885.
18. Foley B, Leitner T, Apetrei C, Hahn B, Mizrachi I, Mullins J, Rambaut A, Wolinsky S, Korber B. HIV Sequence Compendium 2018. Theoretical Biology and Biophysics Group, Los Alamos National Laboratory, NM, LA-UR 18-25673; 2018.
19. Cristian L, Lear JD, DeGrado WF. Determination of membrane protein stability via thermodynamic coupling of folding to thiol-disulfide interchange. Protein science : a publication of the Protein Society 2003;12(8):1732-1740.
20. Furuta RA, Wild CT, Weng Y, Weiss CD. Capture of an early fusion-active conformation of HIV-1 gp41. Nature Structural Biology 1998;5(4):276-279.
21. Ivan B, Sun Z, Subbaraman H, Friedrich N, Trkola A. CD4 occupancy triggers sequential pre-fusion conformational states of the HIV-1 envelope trimer with relevance for broadly neutralizing antibody activity. PLOS Biology 2019;17(1):e3000114.
22. Pancera M, Zhou T, Druz A, Georgiev IS, Soto C, Gorman J, Huang J, Acharya P, Chuang GY, Ofek G and others. Structure and immune recognition of trimeric pre-fusion HIV-1 Env. Nature 2014;514(7523):455-61.
23. Dwyer JJ, Hasan A, Wilson KL, White JM, Matthews TJ, Delmedico MK. The Hydrophobic Pocket Contributes to the Structural Stability of the N-Terminal Coiled Coil of HIV gp41 but Is Not Required for Six-Helix Bundle Formation. Biochemistry 2003;42(17):4945-4953.
24. Marti DN, Bjelić S, Lu M, Bosshard HR, Jelesarov I. Fast Folding of the HIV-1 and SIV gp41 Six-helix Bundles. Journal of Molecular Biology 2004;336(1):1-8.
25. Tatko CD, Nanda V, Lear JD, DeGrado WF. Polar Networks Control Oligomeric Assembly in Membranes. Journal of the American Chemical Society 2006;128(13):4170-4171.
26. Leaman DP, Kinkead H, Zwick MB. In-solution virus capture assay helps deconstruct heterogeneous antibody recognition of human immunodeficiency virus type 1. J Virol 2010;84(7):3382-95.
27. Agrawal N, Leaman DP, Rowcliffe E, Kinkead H, Nohria R, Akagi J, Bauer K, Du SX, Whalen RG, Burton DR and others. Functional Stability of Unliganded Envelope Glycoprotein Spikes among Isolates of Human Immunodeficiency Virus Type 1 (HIV-1). PLoS One 2011;6(6):e21339.